



Published in final edited form as:

J Glaucoma. 2018 November ; 27(11): 957–964. doi:10.1097/IJG.0000000000001042.

Fluorescein Aqueous Angiography in Live Normal Human Eyes

Alex S. Huang¹, Rafaella C. Penteadó², Sajib K. Saha¹, Jiun L. Do², Philip Ngai², Zhihong Hu¹, and Robert N. Weinreb²

¹Doheny Eye Institute and Department of Ophthalmology, David Geffen School of Medicine at UCLA, Los Angeles, CA

²Hamilton Glaucoma Center, Shiley Eye Institute, and Department of Ophthalmology University of California, San Diego, CA

Abstract

Purpose: To evaluate aqueous humor outflow (AHO) in intact eyes of live human subjects during cataract surgery using fluorescein aqueous angiography.

Methods: Aqueous angiography was performed in 8 live human subjects (56 – 86 years old; 2 men and 6 women). After anesthesia, fluorescein (2%) was introduced into the eye (either alone or after indocyanine green [ICG; 0.4%]) from a sterile, gravity-driven constant-pressure reservoir. Aqueous angiographic images were obtained with a Spectralis HRA+OCT and FLEX module (Heidelberg Engineering). Using the same device, anterior segment optical coherence tomography (OCT) and infrared (IR) images were also concurrently taken with aqueous angiography.

Results: Fluorescein aqueous angiography in the live human eye demonstrated segmental AHO patterns. Initial angiographic signal was seen on average by 14.0 +/- 3.0 seconds (mean +/- standard error). Using multi-modal imaging, angiographically positive signal co-localized with episcleral veins (IR imaging) and intrascleral lumens (anterior segment OCT). Sequential aqueous angiography with ICG followed by fluorescein showed similar segmental angiographic patterns.

Discussion: Fluorescein aqueous angiography in live humans was similar to that reported in non-human primates and to ICG aqueous angiography in live humans. As segmental patterns with sequential angiography using ICG followed by fluorescein were similar, these tracers can now be employed sequentially, before and after trabecular outflow interventions, to assess their effects on AHO in live human subjects.

Introduction:

Recently, there has been growing interest to better understand aqueous humor outflow (AHO) pathways.^{1, 2} As traditionally depicted in the literature, conventional AHO moves from the anterior chamber (AC) through the multi-layered trabecular meshwork (TM) and then through Schlemm's canal (SC), collector channels (CC), an intrascleral venous plexus, aqueous veins, and finally into episcleral veins.^{3, 4} However, a variety of structural

assessments and tracer-based studies from post-mortem laboratory animal and human eyes to live humans have now shown that AHO is more complex. Segmental patterns, structural motion, pulsatile flow, and dynamic behaviors have been described.⁵⁻⁸

Structural AHO assessment has focused on SC and nearby CCs. In the laboratory, 3D micro-CT of perfused post-mortem human eyes has shown CC heterogeneity with different configurations, numbers, and localization around SC.^{9, 10} Histological work has demonstrated CC collapse and herniation at high pressure.^{11, 12} Anterior-segment optical coherence tomography (AS-OCT) in *ex vivo* human eyes has shown dynamic motion of SC and CC⁸, and this observation has been confirmed by clinical AS-OCT imaging in live patients.⁷ SC/CC has also been visualized in live humans using AS-OCT with automated image segmentation to build a 3-D representation of outflow pathways.¹³ However, the dependence on histological and OCT evaluation means that investigators are sampling outflow anatomy using tissue or optical slices from the eye. This can be challenging when relevant structures (like CCs) are small so that they can be missed. Also, attempts to circumferentially and comprehensively map AHO pathways around the limbus in live human subjects is possible but laborious and time consuming.¹³ Lastly, no firm relationship exists that translates SC and CC structural configuration to different aqueous humor fluid flow parameters. Therefore, tracer-based studies are an alternative approach that places tracers in the eye to visualize where fluid flows regardless of anatomic detail.

Tracer-based AHO studies were initially conducted *ex vivo* but have now also been employed in the operating room in patients undergoing cataract surgery. Each tracer (gold particles, beads, fluorescein, indocyanine green [ICG], etc.) has unique molecular properties which can impact the final outflow pattern.^{5, 6, 14-25} However, regardless of the tracer, method (bead-based, canalograms, or aqueous angiography), or organism tested (post-mortem mouse, pig, cow, and human or live non-human primate and human), the common final result is that AHO is segmental around the limbus and not circumferentially uniformly distributed.^{5, 6, 14-25} Live aqueous angiography in non-human primates and humans has additionally shown that AHO is pulsatile (consistent with AS-OCT structural work) and possibly related to the cardiac cycle.⁵ Dynamic AHO is another behavior that has been seen. Here, regions that either initially do or do not have tracer-visualized aqueous outflow signal appear to decrease or increase that signal, respectively.^{5, 6}

Here we describe aqueous angiography using fluorescein in live normal human eyes during routine cataract surgery. Aqueous angiography has been published in live humans with ICG,⁶ but the angiographic camera can image two tracers (fluorescein and ICG). In the laboratory, sequential aqueous angiography (using ICG followed by fluorescein) has been performed in cow¹⁶ and human¹⁵ eyes demonstrating similar patterns. This allowed for *ex vivo* interventional testing on the conventional outflow pathways where ICG aqueous angiography was first performed to establish a pattern followed by trabecular bypass and then by fluorescein aqueous angiography to query the effect.¹⁵ Therefore, establishing fluorescein aqueous angiography in live humans creates the same diagnostic paradigm for evaluating conventional outflow interventions in human subjects.

Methods:

Test Subjects:

This study was carried out in accordance with the Declaration of Helsinki and approved by the Institutional Review Board of University of California, San Diego. Written informed consent was obtained. Eight subjects were recruited (Table 1; 6 women and 2 men; 4 right and 4 left eyes; average age = 68.9 years of age (56–86 years-old) with cataracts that included the nuclear sclerotic, posterior subcapsular, or both types. No patient had a history of known fluorescein, ICG, shellfish, or iodine allergy.

Surgical Procedure:

All subjects underwent standard phacoemulsification starting with pre-operative topical dilating (1% tropicamide and 2.5% phenylephrine [Akorn, IL, USA]), antibiotic, and steroid drops followed by lidocaine jelly. Monitored anesthesia care (including intravenous fentanyl and midazolam) was provided followed by surgical time-out, sterile-prep, drape, and placement of a lid speculum. Prior to phacoemulsification surgery, a 1 mm side-port paracentesis was made slightly superior-temporal (right eye) or infero-temporal (left eye) through which a Lewicky AC-maintainer (20g [K20–3276], Katena, NJ, USA) was inserted. Aqueous humor was evacuated with a syringe followed by addition of tracer and imaging (see aqueous angiography below for details). The surgeon would verbally indicate to the imager that tracer delivery was begun to initiate image acquisition. After completing aqueous angiography, the AC-maintainer was removed, tracer irrigated from the anterior chamber, and 1% preservative-free lidocaine added followed by viscoelastic segueing into standard phacoemulsification (Centurion Vision System; Alcon, Ft. Worth, TX, USA). The side-port incision through which the AC-maintainer was inserted doubled as the phacoemulsification second instrument port. Therefore, no additional incisions other than what is routinely required for phacoemulsification were made. All incisions were hydrated and noted to be free of leaks at the conclusion of surgery. After surgery, patients were followed on post-operative day 1, week 1, and month 1 and 3 with standard topical antibiotics and anti-inflammatory drops followed by taper.

Aqueous Angiography

Aqueous angiography imaging was performed as previously described.^{5, 6} The surgical suite was arranged by moving the FLEX module into the operating room. The FLEX module is a modified surgical boom arm that allowed for stable three dimensional manipulations and positioning of the Spectralis HRA+OCT (Heidelberg Engineering GmbH, Heidelberg, Germany) camera head relative to the patient's supine position and eye through the use of multiple pivot joints. Alignment of the OCT/angiographic images along the z-axis was controlled by an integrated micro-manipulator. The FLEX module was situated between the patient's bed and anesthesia station (Fig. 1). This provided a working space for the FLEX operator to the left of the patient. The camera head was surgically draped (Microscope Head Cover [40101.000], Microtek, Dominican Republic) to maintain a sterile environment for imaging. Next to the head rest, an IV pole was sterile-draped (General Purpose Probe Cover [PC1289], Ecolab, MN, USA) and placed on the side of the eye to be imaged. This pole held

a syringe reservoir with a three-way stop cock, situated ~10 inches above the eye, and provided a gravity-delivered constant pressure of ~18.7 mm Hg.

From this position, the camera head was placed above the eye, and confocal scanning laser ophthalmoscopic (cSLO) infrared (IR) images were acquired to center the eye in the picture frame using a 55-degree lens (subjects 1–3 and 7–8; ~25 diopter focus) or anterior segment lens (subjects 4–6; ~37 diopter focus). Subsequently, fluorescence images were obtained using the fluorescein capture mode (excitation wavelength: 486 nm and transmission filter set at > 500 nm) or ICG capture mode (excitation wavelength: 786 nm and transmission filter set at > 800 nm) to establish a pre-injection background that appeared black. Pharmaceutical grade 25% fluorescein (AK-Fluor 25% [NDC17478–25–20], Akorn) was diluted at room temperature in pharmaceutical grade and sterile balanced salt solution (BSS; Alcon) normally used for human cataract surgery to 2.0%. Pharmaceutical grade indocyanine green (ICG, ICGREEN 25 mg [NDC 17478–701–25], Akorn) was thoroughly dissolved with 0.7 ml of the manufacturer provided sterile solvent followed by 5.6 ml of sterile BSS to a final 0.4% ICG concentration. These concentrations were chosen based on prior experience in enucleated cow¹⁶/human¹⁵ eyes, intact/living non-human primate⁵ and human⁶ eyes, and because they have been described for clinical use at these concentrations in live humans as intraocular capsular stains to assist cataract surgery.²⁶ After introduction of tracer, IR and angiographic images were acquired using the FLEX Module with the subject looking in different directions.

Aqueous Angiography Quantitative Assessment

To quantify the angiographic signal, a semi-automated program was developed (Matlab R2018a, Natick, MA) (Fig. 2). After standardizing all pixel intensities to a 0–255 range, using a graphical user interface (GUI), the investigator manually delineated the limbal border for each image. Using this border, the program automatically generated three test lines expanded outward from the limbus at 15, 30, and 45 pixel-increments while maintaining the same curvature. The investigator then manually marked the limbal extent of each quadrant (superior, temporal, inferior, and nasal). The pixel intensities along each test-line (15-line, 30-line, and 45-line) were acquired for each quadrant, smoothed (using a 3×3 averaging window), and plotted over their length. The summative signal intensity for each line was then determined and compared amongst the quadrants. For each quadrant, the signal intensity was divided by the total intensity obtained for each eye to yield a percent signal intensity. Statistical comparison between the quadrant percent signal intensities were made with two-sample, equal-sized, and paired, Student's t-tests (Microsoft Excel 2010). All values are expressed as mean +/-SEM.

Anterior Segment Optical Coherence Tomography (OCT)

Anterior segment OCT (anterior segment module [Heidelberg Engineering, Germany] on Scleral mode) was concurrently acquired in subjects 5 and 6 during fluorescein aqueous angiography to determine if angiographically positive regions showed vessel anatomy compatible for AHO. Single line scans with a 15-degree scan angle (3.9-micron axial and 11-micron lateral resolution; ~ 4.5 mm) were taken with oversampling (automated real-time setting = 3).

Results:

Similar to post-mortem eyes (using fluorescein and ICG)^{14–16} and intact eyes from non-human primates (using fluorescein and ICG)⁵ and live humans (using ICG),⁶ fluorescein aqueous angiography in intact eyes of living human subjects undergoing cataract surgery showed increasing signal over time (Fig. 3; Subject 1) with segmental patterns (Fig. 4; Subjects 1–3). Initial angiographic signal was seen on average by 14.0 \pm 3.0 seconds with a range from 4 – 24 seconds. Qualitatively, angiographic signal was usually more prominent nasally although focal regions with low nasal angiographic AHO could be seen (Fig. 4; Subject 2 [row A] and Subject 3 [row C]). Temporal angiographic signal, ranging from minimal to significant, could be seen as well (Fig. 4; rows A/B/C).

Quantitatively, angiographic signal was measured in 4 subjects (Subjects 1–3 and 7). Signal intensity was obtained from three test lines at 15, 30, and 45 pixel-increments from the limbus that maintained the same curvature (Fig. 2). Overall the 15-line showed the greatest relative signal intensity (15-line: 45 \pm 5.5%; 30-line: 32.7 \pm 3.7%; and 45-line: 22.3 \pm 2.9% of the total signal intensity for all three lines combined per eye). Therefore, for quadrant comparisons, the 15-line was used. Comparing the quadrants, the nasal quadrant had the greatest and the temporal quadrant had the least relative signal intensity (nasal: 45.1 \pm 4.6%; temporal 9.1 \pm 1.3%; superior 22.7 \pm 9.0%, and inferior 23.0 \pm 6.7%). In pairwise comparisons, the only statistically significant differences were found between the nasal and temporal quadrants ($p = 0.009$) and the nasal and inferior quadrants ($p = 0.028$).

To validate aqueous angiography signal as compatible with AHO, fluorescein aqueous angiography was performed in conjunction with IR imaging and OCT. Fluorescein aqueous angiography showed similar patterns to episcleral veins on IR imaging (Fig. 5; Subjects 3 and 4). This was more easily appreciated in regions of less intense aqueous angiographic signal as angiographic structures were more delineated. Supporting this, anterior segment OCT in angiographically positive regions also demonstrated strikingly more and larger intrascleral lumens compatible for AHO compared to angiographically negative regions (Fig. 6; Subjects 5 and 6).

Previously, aqueous angiography had been conducted in sequence with ICG prior to fluorescein in the laboratory^{15, 16} or in live non-human subjects.⁵ Therefore, we performed the same imaging sequence here in live humans. Comparable results were seen here in live humans between ICG and fluorescein where ICG aqueous angiography (performed first) showed nearly identical segmental high- and low-signal patterns to fluorescein aqueous angiography (performed second) in the same eyes (Fig. 7; Subjects 7 and 8).

Discussion:

Fluorescein aqueous angiography showed segmental angiographic patterns, similar to prior reports using ICG and fluorescein in non-human primates⁵ and ICG alone in humans.⁶ AS-OCT and CSLO IR imaging combined with fluorescein aqueous angiography confirmed that the fluorescein signal was compatible with AHO. Importantly, just like in living non-human

primates,⁵ fluorescein aqueous angiography showed very similar patterns to that of ICG in the same eye when performed sequentially.

The purpose of this study was to describe fluorescein aqueous angiography in a small number of live human eyes. Advantages of fluorescein over ICG is that it is less expensive and more likely to be available in eye care clinics given more frequent use of retinal fluorescein intravenous angiography over that of ICG.²⁷ Also, fluorescein is well-tolerated without iodine-allergy sometimes seen with ICG. Therefore, if clinically helpful and performed in a single application, aqueous angiography with fluorescein may be more widely used than with ICG.²⁸

Alternatively, ICG has its own advantages given its larger molecular weight, longer excitation and emission wavelengths, and propensity to be protein bound. In the posterior pole, while both ICG and fluorescein are suitable for retinal vascular angiography, ICG's characteristics make it more suitable for choroidal angiography.²⁷ Translated to the anterior segment, ICG's characteristics allow for greater AHO intraluminal retention and less leakage compared to fluorescein. Also, ICG could theoretically image AHO pathways slightly deeper than fluorescein given greater depth of penetration based on its longer excitation/emission wavelengths.

Sequentially, ICG angiography followed by fluorescein angiography showed very similar but not identical patterns. This supports results from post-mortem bovine¹⁶ and human¹⁵ eyes as well as those seen in live non-human primates.⁵ Differences likely come from the subtle molecular dissimilarities between the tracers (see above). Laboratory testing has shown that at these concentrations, ICG angiography should precede fluorescein, because in the presence of ICG, fluorescein can demonstrate some emission using ICG-based excitation wavelengths and filters.¹⁶ With this method in place, sequential angiography can now be used to test outflow interventions such as trabecular bypass or new conventional outflow drugs in live humans by performing ICG angiography to establish a baseline and then fluorescein angiography after an intervention to query the impact.

While the literature for conventional/trabecular aqueous angiographic imaging is growing, consideration can also be made for uveoscleral aqueous angiography as well although challenges exist. First, the uveoscleral outflow pathway is deeper so that it may be hard to image angiographically due to scleral diffraction of fluorescent emission. Second, conventional outflow resides more superficial to uveoscleral outflow so that even if uveoscleral outflow aqueous angiography was possible, it could be blocked by more superficial aqueous angiography of the conventional pathway. Therefore, aqueous angiography attempts for uveoscleral outflow in temporal or low-signal regions may be the best place to start. Also, large uveoscleral outflow correlates (such as lakes or clefts from trauma or uveoscleral minimally invasive glaucoma surgeries²⁹) might concentrate the tracer to further facilitate initial attempts at uveoscleral angiographic imaging.

This study has similar limitations to prior aqueous angiographic reports where the method requires a lid speculum that could have impacted the ocular surface, and aqueous angiography continues to be invasive. Additionally, the sample size was small which made it

difficult to determine if individual differences impacted AHO. This included gender, sex, and race. Their role in AHO would make for important future study. Also, the patients had a mixture of medical co-morbidities including hypertension, diabetes, and hyperlipidemia. While we were restricted to imaging only those patients who needed routine cataract surgery, it would also be interesting to study the relationship between certain diseases, particularly vascular, to AHO.

In conclusion, fluorescein aqueous angiography in live and normal human eyes continues to support segmental AHO. In studying AHO, many tracers have been reported with overall comparable results between the laboratory and clinical setting.^{5, 6, 14–25} Tracer characteristics lend to certain advantages when imaging for different purposes. Similar angiographic patterns seen during sequential imaging of the same eye using two tracers now allows for future angiographic evaluation of conventional outflow surgeries or drugs in live humans.

Acknowledgements

Funding for this work came from National Institutes of Health, Bethesda, MD (Grant Numbers K08EY024674 [ASH] and R01EY029058 [RNW]; Research to Prevent Blindness Career Development Award 2016 [ASH]; and an unrestricted grant from Research to Prevent Blindness [UCLA and UCSD] (New York, NY).

References:

1. Huang AS, Mohindroo C, Weinreb RN. Aqueous Humor Outflow Structure and Function Imaging At the Bench and Bedside: A Review. *J Clin Exp Ophthalmol* 2016;7(4).
2. Huang AS, Francis BA, Weinreb RN. Structural and functional imaging of aqueous humour outflow: a review. *Clin Exp Ophthalmol* 2018;46(2):158–68. [PubMed: 28898516]
3. Johnson M ‘What controls aqueous humour outflow resistance?’. *Exp Eye Res* 2006;82(4):545–57. [PubMed: 16386733]
4. Swaminathan SS, Oh DJ, Kang MH, Rhee DJ. Aqueous outflow: segmental and distal flow. *J Cataract Refract Surg* 2014;40(8):1263–72. [PubMed: 25088623]
5. Huang AS, Li M, Yang D, et al. Aqueous Angiography in Living Nonhuman Primates Shows Segmental, Pulsatile, and Dynamic Angiographic Aqueous Humor Outflow. *Ophthalmology* 2017.
6. Huang AS, Camp A, Xu BY, et al. Aqueous Angiography: Aqueous Humor Outflow Imaging in Live Human Subjects. *Ophthalmology* 2017.
7. Li P, Shen TT, Johnstone M, Wang RK. Pulsatile motion of the trabecular meshwork in healthy human subjects quantified by phase-sensitive optical coherence tomography. *Biomed Opt Express* 2013;4(10):2051–65. [PubMed: 24156063]
8. Li P, Reif R, Zhi Z, et al. Phase-sensitive optical coherence tomography characterization of pulse-induced trabecular meshwork displacement in ex vivo nonhuman primate eyes. *J Biomed Opt* 2012;17(7):076026. [PubMed: 22894509]
9. Bentley MD, Hann CR, Fautsch MP. Anatomical Variation of Human Collector Channel Orifices. *Invest Ophthalmol Vis Sci* 2016;57(3):1153–9. [PubMed: 26975026]
10. Hann CR, Bentley MD, Vercnocke A, et al. Imaging the aqueous humor outflow pathway in human eyes by three-dimensional micro-computed tomography (3D micro-CT). *Exp Eye Res* 2011;92(2):104–11. [PubMed: 21187085]
11. Hann CR, Vercnocke AJ, Bentley MD, et al. Anatomic changes in Schlemm’s canal and collector channels in normal and primary open-angle glaucoma eyes using low and high perfusion pressures. *Invest Ophthalmol Vis Sci* 2014;55(9):5834–41. [PubMed: 25139736]
12. Battista SA, Lu Z, Hofmann S, et al. Reduction of the available area for aqueous humor outflow and increase in meshwork herniations into collector channels following acute IOP elevation in bovine eyes. *Invest Ophthalmol Vis Sci* 2008;49(12):5346–52. [PubMed: 18515571]

13. Huang AS, Belghith A, Dastiridou A, et al. Automated circumferential construction of first-order aqueous humor outflow pathways using spectral-domain optical coherence tomography. *J Biomed Opt* 2017;22(6):66010. [PubMed: 28617922]
14. Saraswathy S, Tan JC, Yu F, et al. Aqueous Angiography: Real-Time and Physiologic Aqueous Humor Outflow Imaging. *PLoS One* 2016;11(1):e0147176. [PubMed: 26807586]
15. Huang AS, Saraswathy S, Dastiridou A, et al. Aqueous Angiography-Mediated Guidance of Trabecular Bypass Improves Angiographic Outflow in Human Enucleated Eyes. *Invest Ophthalmol Vis Sci* 2016;57(11):4558–65. [PubMed: 27588614]
16. Huang AS, Saraswathy S, Dastiridou A, et al. Aqueous Angiography with Fluorescein and Indocyanine Green in Bovine Eyes. *Transl Vis Sci Technol* 2016;5(6):5.
17. Keller KE, Bradley JM, Vranka JA, Acott TS. Segmental versican expression in the trabecular meshwork and involvement in outflow facility. *Invest Ophthalmol Vis Sci* 2011;52(8):5049–57. [PubMed: 21596823]
18. Vranka JA, Bradley JM, Yang YF, et al. Mapping molecular differences and extracellular matrix gene expression in segmental outflow pathways of the human ocular trabecular meshwork. *PLoS One* 2015;10(3):e0122483. [PubMed: 25826404]
19. Hann CR, Bahler CK, Johnson DH. Cationic ferritin and segmental flow through the trabecular meshwork. *Invest Ophthalmol Vis Sci* 2005;46(1):1–7. [PubMed: 15623746]
20. Braakman ST, Read AT, Chan DW, et al. Colocalization of outflow segmentation and pores along the inner wall of Schlemm’s canal. *Exp Eye Res* 2015;130:87–96. [PubMed: 25450060]
21. Cha ED, Xu J, Gong L, Gong H. Variations in active outflow along the trabecular outflow pathway. *Exp Eye Res* 2016.
22. Swaminathan SS, Oh DJ, Kang MH, et al. Secreted protein acidic and rich in cysteine (SPARC)-null mice exhibit more uniform outflow. *Invest Ophthalmol Vis Sci* 2013;54(3):2035–47. [PubMed: 23422826]
23. Chang JY, Folz SJ, Laryea SN, Overby DR. Multi-scale analysis of segmental outflow patterns in human trabecular meshwork with changing intraocular pressure. *J Ocul Pharmacol Ther* 2014;30(2–3):213–23. [PubMed: 24456518]
24. Grieshaber MC, Pienaar A, Olivier J, Stegmann R. Clinical evaluation of the aqueous outflow system in primary open-angle glaucoma for canaloplasty. *Invest Ophthalmol Vis Sci* 2010;51(3):1498–504. [PubMed: 19933180]
25. Zeppa L, Ambrosone L, Guerra G, et al. Using canalography to visualize the in vivo aqueous humor outflow conventional pathway in humans. *JAMA Ophthalmol* 2014;132(11):1281. [PubMed: 25188749]
26. Jacobs DS, Cox TA, Wagoner MD, et al. Capsule staining as an adjunct to cataract surgery: a report from the American Academy of Ophthalmology. *Ophthalmology* 2006;113(4):707–13. [PubMed: 16581432]
27. Keane PA, Sadda SR. Imaging chorioretinal vascular disease. *Eye (Lond)* 2010;24(3):422–7. [PubMed: 20010789]
28. Burke M Indocyanine green dye for choroidal angiography. *J Ophthalmic Nurs Technol* 1996;15(5):186–9. [PubMed: 9120865]
29. Vold S, Ahmed II, Craven ER, et al. Two-Year COMPASS Trial Results: Supraciliary Microstenting with Phacoemulsification in Patients with Open-Angle Glaucoma and Cataracts. *Ophthalmology* 2016;123(10):2103–12. [PubMed: 27506486]

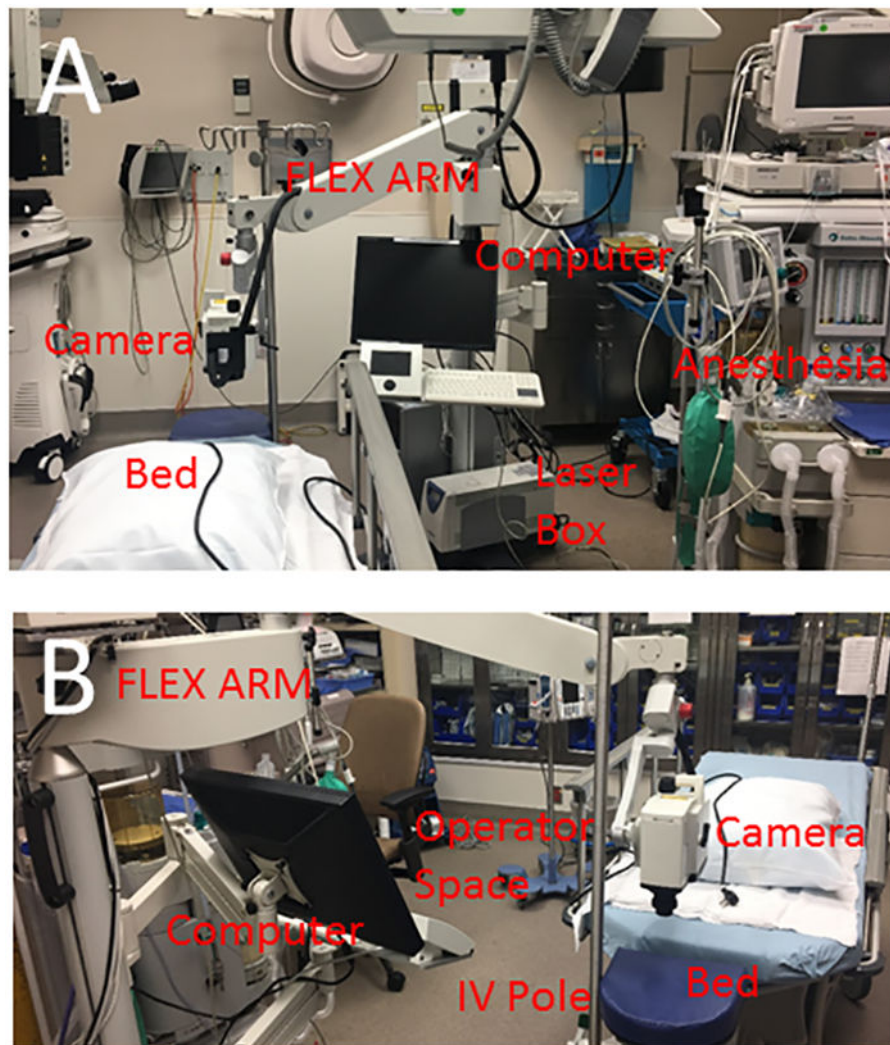


Figure 1.

Aqueous Angiography Setup in the Operating Room

A) The Heidelberg FLEX module is a modified surgical boom integrated with all components of the Spectralis (HRA+OCT) including the computer, laser box, and camera head. The FLEX module is situated near the head of the bed between the bed and anesthesia work space. B) This leaves a space for the FLEX module operator to operate the device next to the patient. An IV pole is placed near the head of the bed for the tracer reservoir.

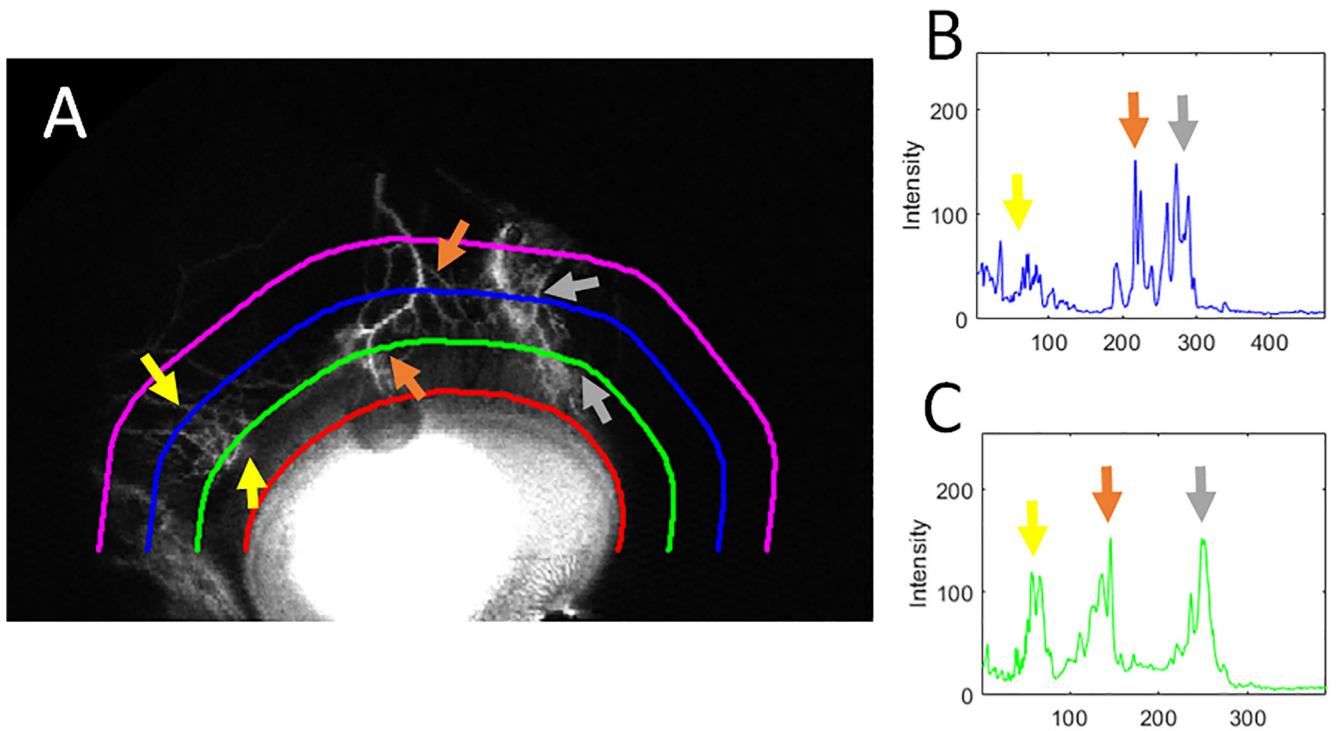


Figure 2.

Quantitative Assessment of Angiographic Signal

A) For each quadrant (here superior), the limbal border was manually delineated (red line). From this, signal intensity was obtained from three test lines (at 15 [green], 30 [blue], and 45 [purple] pixel-increments from the limbus while maintaining the same shape). B) Plotted over its length, the 30-line (blue) shows distinct peaks. C) Plotted over its length, the 15-line (green) shows even more distinct and larger peaks. Thus, the summative signal intensity was determined for all images using the 15-line and compared between quadrants.

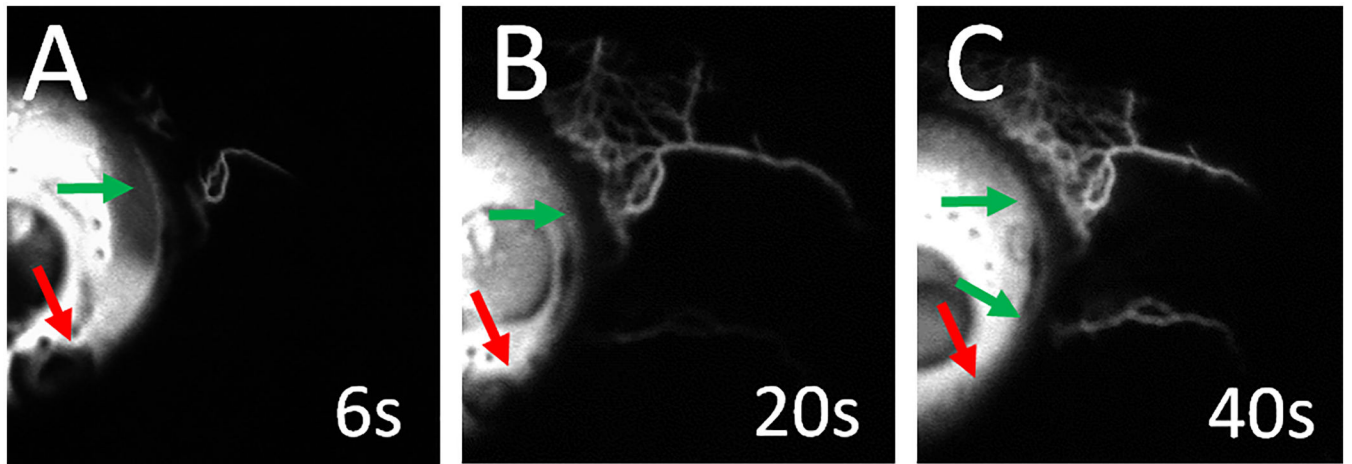


Figure 3.
Fluorescein Aqueous Angiography Signal Development
Subject 1 (right eye; nasal hemisphere) demonstrates increasing fluorescein aqueous angiographic signal (green arrows) over time. Segmental regions of low angiographic signal are also seen (red arrows). White “s” = seconds after tracer introduction.

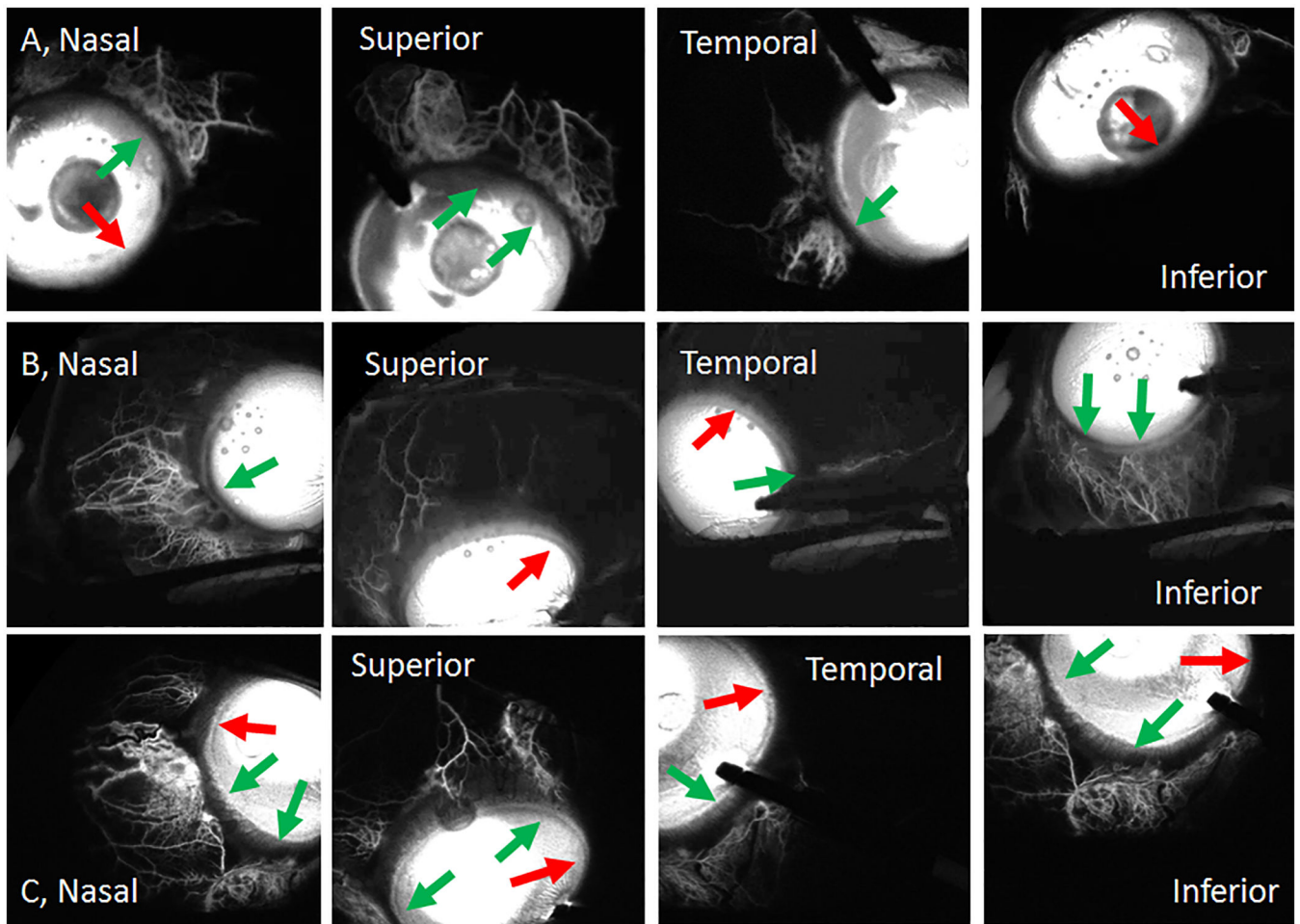


Figure 4.

Fluorescein Aqueous Angiography Shows Segmental Outflow Patterns

Aqueous angiography in different positions of gaze for subject 1 (Row A; right eye, 24–47 seconds), subject 2 (Row B; left eye, 92–103 seconds) and subject 3 (Row C; left eye, 46–56 seconds). Green arrows identify areas with segmental angiographic signal and red arrows point out segmental regions without angiographic signal. Notice that more overall nasal angiographic signal is seen although some temporal signal is observed. The time ranges represent the time it took to take the first and last image for each patient while looking in different directions. Variation in how much time it took and the time the first image was taken had to do with individual differences in addition to patient compliance (due to dilation and sedation) to take and hold eccentric gazes.

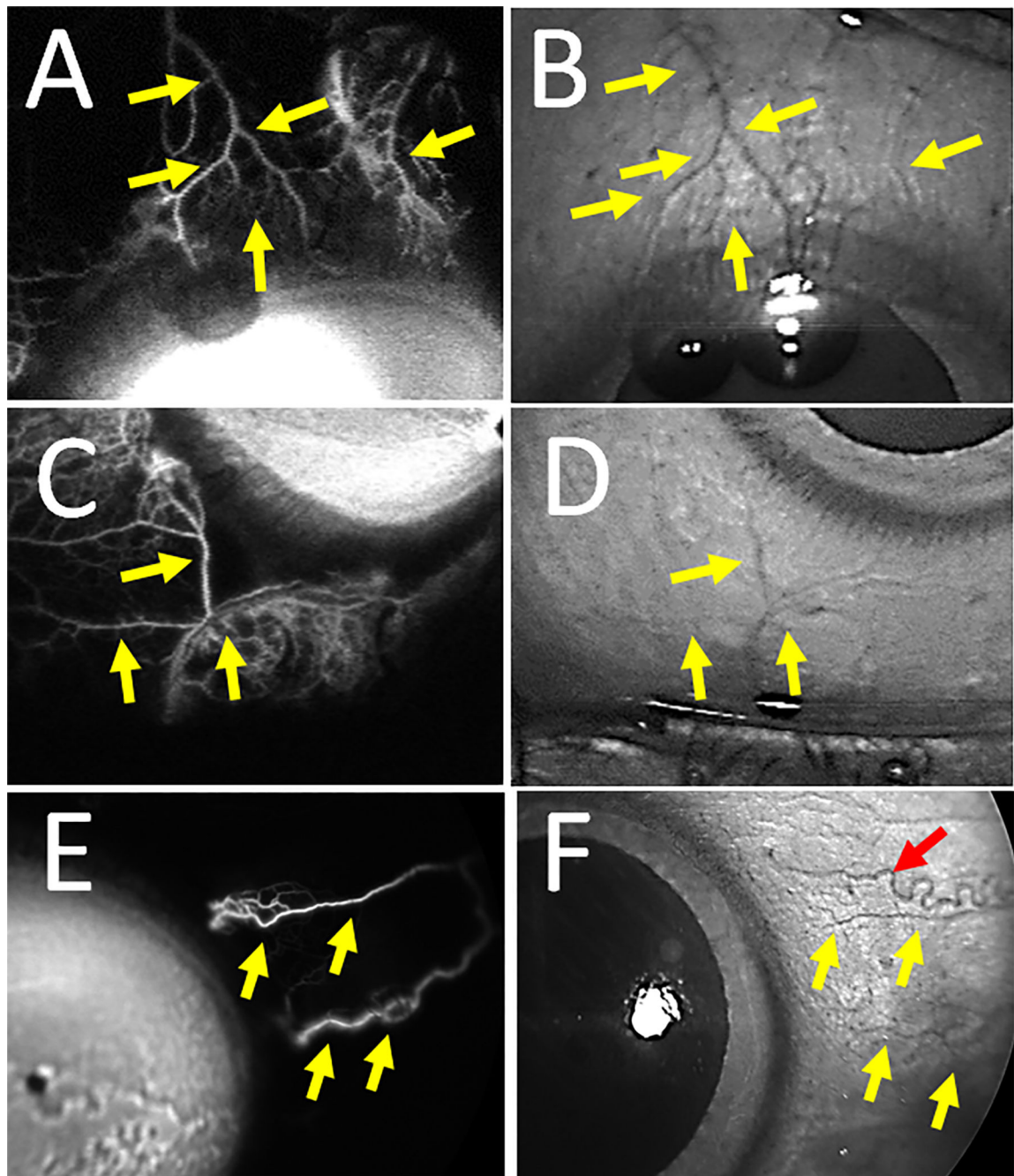


Figure 5.

Fluorescein Aqueous Angiographic Signal Overlaps Episcleral Veins.

A) Aqueous angiographic and (B) CSLO IR images of the superior region of subject 3's left eye showed overlap between angiographic structures and episcleral veins (yellow arrows). C) Aqueous angiographic and (D) CSLO IR images of the inferior nasal region of subject 3's left eye showed overlap between angiographic structures and episcleral veins (yellow arrows). E) Aqueous angiographic and (F) CSLO IR images of the nasal region of subject

4's right eye showed overlap between angiographic structures and episcleral veins (yellow arrows). F) A red arrow points out a corkscrew conjunctival vessel.

Author Manuscript

Author Manuscript

Author Manuscript

Author Manuscript

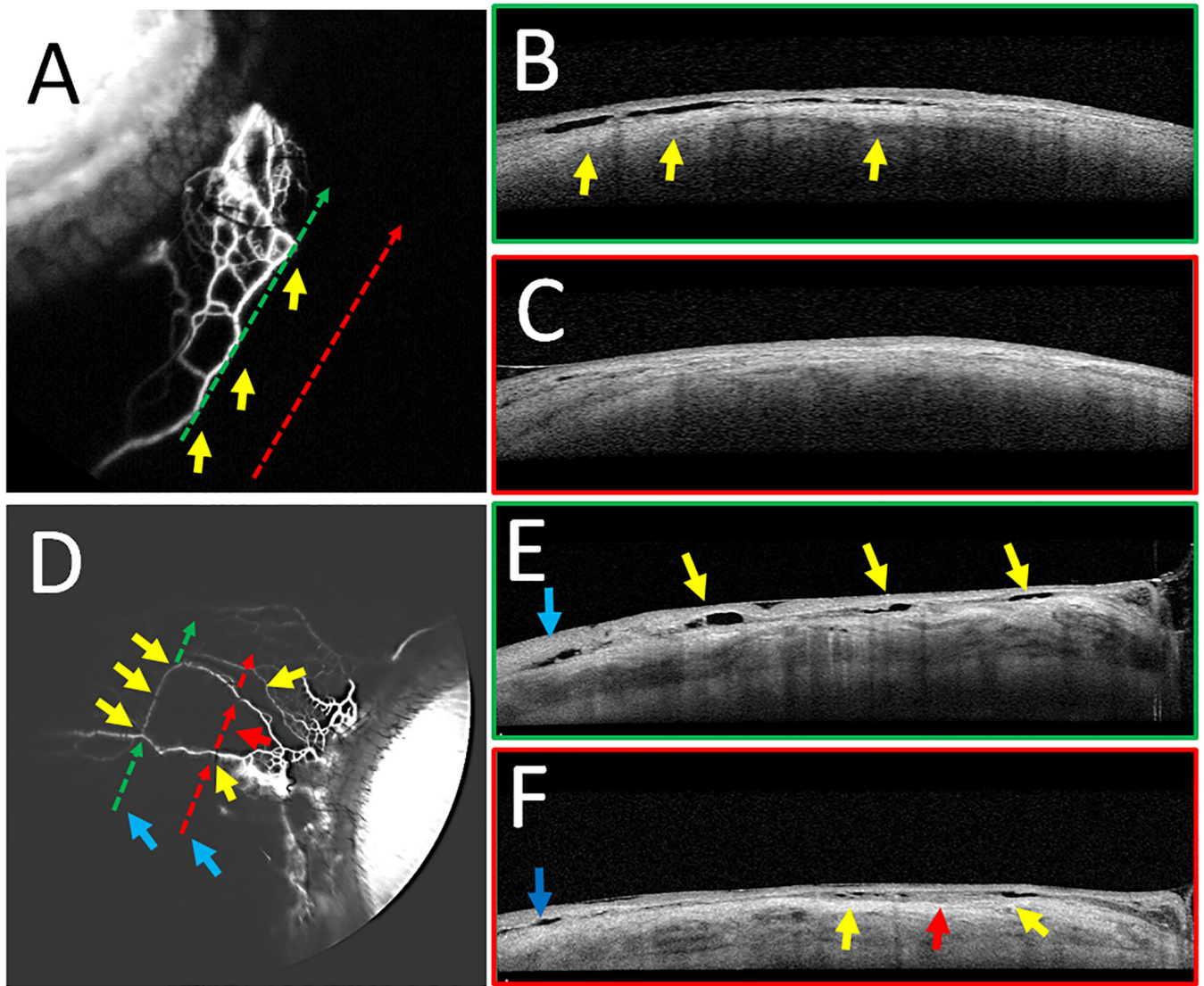


Figure 6.

Fluorescein Aqueous Angiography with Concurrent Anterior Segment OCT

Aqueous angiography with anterior segment OCT was performed on subjects 5 (A-C) and 6 (D-F). B/E) OCT (green dotted arrows in A/D) was performed on a regions of high angiographic signal showing intrascleral lumens capable of carrying aqueous humor. Yellows arrows showed correspondence of angiographic signal (A/D) to OCT lumens (B/E). C/F) OCT (red dotted arrows in A/C) was performed on regions without angiographic signal, demonstrating fewer intrascleral lumens (C/F). E/F) Blue arrows on OCT demonstrate lumens not associated with the aqueous angiographic signal that may be related to other luminal structures in the sclera such as arteries or episcleral veins not associated with AHO. In subject 6, given the thinner nature of the angiographic structures, the arrows were broken to avoid covering them.

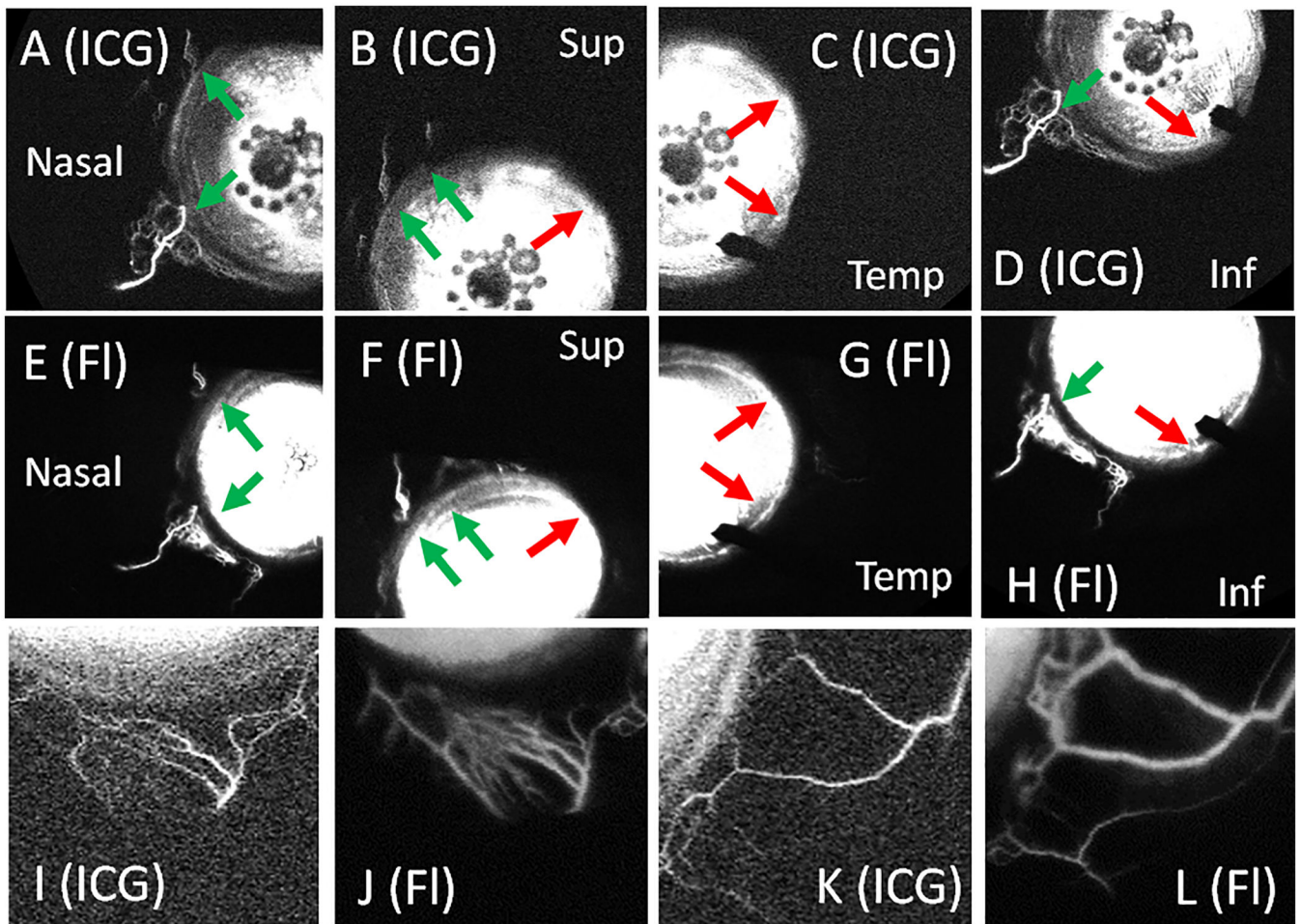


Figure 7. Sequential Aqueous Angiography using ICG Followed by Fluorescein Demonstrates Similar Patterns.

Aqueous angiography was performed in subject 7 using ICG (A-D) followed by fluorescein (E-H) in the same left eye. (A-D) ICG aqueous angiography showed segmental regions with (green arrows) and without (red arrows) angiographic signal that were similar to the patterns obtained using fluorescein (E-H). ICG signal started at 9 seconds and fluorescein signal started at 4 seconds. A closer view of subject 8's inferior (I) and nasal (K) regions using ICG also showed similar patterns to that obtained with fluorescein (J and L). ICG = indocyanine green. Fl = fluorescein. Temp = temporal. Sup = superior. Inf = inferior.

Table 1.

Characteristics of Subjects

Subject Number	Age	Race	Sex	Eye	Relevant PMH/POH
1	75	Asian	F	Right	Hypertension, h/o Toxoplasmosis Chorioretinitis
2	72	Asian	F	Left	Diabetes
3	67	Caucasian	F	Left	Ptosis Repair
4	59	Caucasian	M	Right	Atrial Fibrillation, Dry Macular Degeneration
5	75	Caucasian	M	Right	Skin Cancer
6	67	Caucasian	F	Left	Breast Cancer, Hyperlipidemia, Hypothyroid
7	86	Asian	F	Left	Hyperlipidemia, Arthritis
8	56	Hispanic	F	Right	Gestational Diabetes

Author Manuscript

Author Manuscript

Author Manuscript

Author Manuscript